SURFACE CLUSTER MODELS FOR V_2O_5 – STUDIES OF THE IMPORTANCE OF LOCAL GEOMETRY

Malgorzata WITKO[a1], Renata TOKARZ[a2] and Klaus HERMANN[b]

[a] *Institute of Catalysis and Surface Chemistry, Polish Academy of Sciences, ul. Niezapominajek, 30 239 Cracow, Poland; e-mail: [1] ncwitko@cyf-kr.edu.pl, [2] nctokarz@cyf-kr.edu.pl*

[b] *Fritz-Haber-Institut der Max-Planck-Gesellschaft, Faradayweg 4–6, D-14 195 Berlin, Germany; e-mail: hermann@handel.RZ-Berlin.MPG.de*

Received May 7, 1998
Accepted June 15, 1998

Dedicated to Professor Rudolf Zahradnik on the occasion of his 70th birthday.

Catalytic properties of the vanadium pentoxide (010) surface are discussed based upon semiempirical quantum chemical calculations using cluster models. Special attention is paid to the role of the second layer in discussing the geometrical factor by using the semiempirical ZINDO approach. Local electronic properties near the different surface oxygen sites are analyzed with the help of Mulliken populations and Meyer bond order indices. Different optimization procedures (with various boundary conditions) are performed for diverse V–O clusters modeling one and two layers. Electronic parameters of the clusters are found to be similar for the cluster in the bulk and optimized geometry. The optimized geometry of the cluster remains much closer to the surface geometry when the optimization is done for the whole cluster, excluding the saturated hydrogen atoms. Optimization of the small fragment of the cluster, results in the significant rearrangement of the cluster structure and leads to the "warped" geometry (bridging oxygen as well as vanadium atoms are shifted out of the surface). Two types of boundary conditions assumed during the optimization process lead to similar results, the optimization of all atoms in the cluster (with saturating hydrogen atoms kept frozen) and the same optimization in the presence of the second layer. The presence of the second layer stabilizes the surface geometry. The role of the second layer is also shown in a formation of an oxygen vacancy at the bridging position.

Key words: Vanadium oxide; V_2O_5; Cluster model calculations; Local geometries; ZINDO; Semiempirical calculations.

The understanding of catalytic processes occurring on transition metal oxide surfaces requires a detailed knowledge of the physical and chemical properties of the surface, a characterization of the transition complex which is formed at the surface, and a description of the elementary steps of the reaction between the adsorbates. The electronic structure of the surface is responsible for the interaction and binding with an adsorbate, the resulting bond changes, the reaction of adsorbed reactant(s), and the desorption process. Therefore, one has to determine which atoms act as active centers directing the

transformation of the reagent and how the properties of the active center depend on its geometrical and chemical arrangements. Furthermore, it is necessary to learn how binding in the intermediate complex (composed of the reacting molecule and a group of atoms of the catalyst forming the active center) modifies the electronic structure of the molecule and influences the reactivity of different bonds, thus determining the type of product. One needs to determine the role of the steric (the mutual orientation of the reacting molecule and the surface) and the electronic factor (the electronic structure of the surface or/and the electronic state of the reacting molecule), and to know how they affect the reaction pathway and hence the type of products.

Nowadays, theoretical approaches, used in parallel or as complementary to surface experimental techniques, allow one to get a wide spectrum of information concerning details of catalytic reactions on both atomic and electronic levels. All theoretical treatments of catalytic systems are based on models. The quality of the theoretical results and their relevance with respect to experimental data for real catalytic systems is determined by basically two approximations, those used to simplify the system geometry and those used to evaluate the electronic structure of the model system. Both approximations influence each other and there are no simple criteria to select a cluster geometry or a theoretical method to yield a given accuracy for the comparison with the experimental results.

The interest in the electronic structure of vanadium oxide surfaces originates from the wide application of vanadia based materials as catalysts, especially in the selective oxidation of hydrocarbons (aliphatic as well as aromatic)[1,2]. The existence of the structurally (and thus electronically) different oxygen sites on the V_2O_5 (010) surface poses the question as to which of these sites is involved in the different elementary steps of the oxidation reaction. In particular, it is interesting to ask which surface oxygen sites are responsible for the activation of C–H bonds (abstraction of hydrogen) in a hydrocarbon reactant near the surface and which is being inserted into the organic molecule (yielding the oxygenated product). Many microscopic details of these processes (which involve adsorption and surface bond breaking/making) are still under discussion and require more experimental as well as theoretical work.

The electronic structure of the vanadium pentoxide (010) surface as well as adsorption at this surface have already been examined[3–17] in different cluster model studies using *ab initio* Hartree–Fock[3–5] and density functional theory[6–8,17] as well as semiempirical INDO (refs[9–14]) and charge sensitivity analysis[15,16] approaches. Most of these studies have been performed using an idealized V_2O_5 (010) surface geometry with averaged interatomic V–O distances and O–V–O angles. The clusters with the bulk geometry have already been examined[8,13,17]. The results show pronounced differences between the structurally different oxygen sites present at the V_2O_5 (010) surface. It is found that bridging oxygen sites are more negatively charged than terminal (vanadyl) sites. Further, hydrogen/proton adsorption at the different oxygen sites always results in

a strong binding and surface OH formation. However, OH groups deriving from doubly coordinated bridging oxygen sites at V_2O_5 (010) can become mobile and can desorb from the surface, whereas terminal OH groups forming above vanadium centers are very tightly bound.

In the following, the catalytic properties of the vanadium pentoxide (010) surface is discussed based upon semiempirical quantum chemical calculations using cluster models. Special attention is paid to the role of the second layer in discussing the geometrical factor in the semiempirical ZINDO approach. Different optimization procedures (with various boundary conditions) are performed for $V_2O_9H_8$, $V_{10}O_{31}H_{12}$, and $V_{24}O_{71}H_{12}$ clusters modeling only one layer as well as for $V_{12}O_{40}H_{20}$ ($V_2O_9H_8$ + $V_{10}O_{31}H_{12}$) and $V_{20}O_{62}H_{24}$ ($V_{10}O_{31}H_{12}$ + $V_{10}O_{31}H_{12}$) clusters modeling two layers. As a next step, the formation of an oxygen vacancy from the bridging oxygen sites is studied.

THEORETICAL

Models

In heterogeneous catalysis two geometric models (cluster models and repeated slab/bulk models) that approximate the real catalyst from the opposite directions are most commonly applied. The basis of the *cluster model*, in which the substrate atoms are cut out of the surface/bulk of the catalyst, is the assumption of a localized interaction near the adsorption site. The surface cluster is treated as a fictitious molecule, with or without additional boundary conditions, to take the effect of environmental coupling into account. Surface clusters are selected according to their size, detailed geometry, and may exhibit different local states. The main drawback of this model is the incorrect treatment of atoms at the cluster periphery, known as the embedding problem. This disadvantage manifests itself in the dependence of the calculated physical and chemical parameters on the size and geometry of the surface[18]. The *repeated slab/bulk model*[19] treats the surface as an infinite system with full translational periodicity. The adsorbate molecules (reactants) form two-dimensional periodic arrangements on the surface (supercell geometry). The periodicity constraints may lead to artificially strong coupling between the adsorbate molecules. This problem could be avoided by using very large supercells. However, one has to achieve a balance between the computational effort and the cell sizes.

Theoretical Methods

The quantum chemical methods used to study catalytic system can be classified into *ab initio* methods (for a quantitative account of small model systems) and semiempirical methods (for obtaining qualitative trends in large model systems). Amongst the *ab initio* methods, two approaches, namely the Hartree–Fock[20] (HF) and the Density Functional

Theory[21] (DFT) are most widely used. Both *ab initio* treatments yield highly accurate electronic states and potential energy surfaces with minima (characterizing reactants, intermediates, and products) and saddle points (describing transitions). The computational effort connected with these methods allows one to treat relatively small cluster systems accurately which may restrict studies to fragments of catalytic systems. The various semiempirical methods[22] are based on the same formalism as the *ab initio* HF method. However, the electron interaction integrals entering the variational equations (which are calculated exactly in the *ab initio* techniques) are approximated by experimental data or adjustment to *ab initio* results. This procedure yields less accurate electronic states and potential energy surfaces compared to those of *ab initio* techniques, but allows semiquantitative studies of much larger clusters which can be sufficient to account for complete real catalytic systems.

When choosing local clusters to model the surface, one has to examine different clusters varying in size and shape in order to assess the cluster size convergence resulting in a reasonable surface representation. In addition, systematic studies using different electronic structure methods (which are complementary in nature) are needed to obtain a complete electronic description of the catalytic model system.

CATALYTIC PROPERTIES OF THE V_2O_5 (010) SURFACE

Crystal Structure of V_2O_5

The crystal lattice of vanadium pentoxide, V2O5, has an orthorhombic symmetry with a space group D_{2h}–P_{mmn} and unit cell parameters defined as a = 11.51 Å, b = 4.37 Å, c = 3.56 Å (refs[23–25]). The building unit of V_2O_5 forms a distorted octahedron with V–O bond distances varying between very short (1.58 Å, vanadyl groups) and very long values (2.79 Å). Such a significant difference in distances allows one to regard the coordination of the vanadium as tetragonal, square pyramidal or octahedral, depending on the extent of the first coordination sphere. Assuming octahedral coordination, each of the oxygens of the vanadyl group (with shortest V–O bond) is also connected by a very long *trans*-bond with a neighboring vanadium. This geometry results in a layer structure with an easy cleavage plane perpendicular to the *b* axis ((010) direction). The lattice of vanadium pentoxide may also be described by zig-zag chains of edge-sharing octahedra running along the *c* axis and crosslinked by shared oxygen corners to form infinite layers in the *ac* plane. Adjacent layers are connected (along the *b* direction) by oxygen corners involving both very long and very short V–O distances. Therefore, the catalytically active (010) surface of V_2O_5 can be discussed in terms of distorted edge and corner linked square pyramids. This surface contains three structurally different oxygen sites, vanadyl oxygens coordinated to one vanadium, O(1), and bridging oxygens coordinated to two, O(2), or three, O(3), vanadium atoms. When the adsorbate molecule is involved, the situation is even more complex and one can distinguish five

structurally inequivalent surface oxygens O(a–e), the vanadyl oxygen O(a)≡O(1) coordinated to one vanadium, bridging oxygens O(b,c)≡O(2) coordinated to two vanadiums, where O(b) bridges two vanadyl groups whereas O(c) connects two bare vanadium atoms, and bridging oxygens O(d,e)≡O(3) coordinated to three vanadiums but involving vanadyl groups with different orientations (Fig. 1).

In the following, the (010) surface of V_2O_5 is modeled by clusters of finite size where the electronic structure and respective geometry optimization are determined by the semiempirical ZINDO method[26–28]. Local electronic properties near the different surface oxygen sites are analyzed with the help of Mulliken populations and Meyer bond order indices.

Electronic and Geometric Structure of V_2O_5 Surface Clusters

Standard methods of quantum chemistry (originally developed to treat individual, isolated molecules) consider the model cluster and the adsorbed molecule as parts of a single supermolecule where all the interactions are treated on an equal footing. One has to mention that, in the case of semiempirical methods (parametrized in a way to form typical chemical bonds) free chemical interactions (without any boundary conditions) between the reactants and the catalyst substrate or among the atoms constituting the surface cluster, lead to the formation of unrealistic supermolecules. These supermolecules do not preserve the geometry of the surface. This conclusion that the geometry of the surface cluster after optimization does not resemble the surface geometry goes against the cluster model approximation, assuming that the cluster cut out of the surface simulates the surface. On the other hand, it is necessary to study free chemical interactions between two parts of the supermolecule in order to consider that they both have to rearrange themselves according to the operating chemical forces. The incoming adsorbing molecule “feels” the presence of the surface already at a large distance, but also the model surface cluster examines the presence of the adsorbate. Thus both partners influence each other and such a mutual interaction has to be analyzed. The problem to

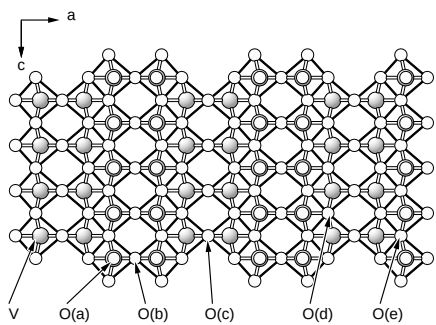

FIG. 1
Geometric structure of the (010) crystal plane of V_2O_5 where V(O) centers are included as shaded (white) balls and the different surface oxygen sites O(a–e) are labelled

be solved consists in examining the boundary conditions assumed during the geometry optimization. Therefore, in the following, different types of optimization conditions are discussed.

The vanadium pentoxide structure is modeled by V–O clusters cut out of the bulk and saturated by hydrogen atoms positioned along the direction to the nearest vanadium center in such way that they form OH groups. The following clusters are selected: $V_2O_9H_8$, $V_{10}O_{31}H_{12}$, and $V_{24}O_{71}H_{12}$ clusters describing one layer (Fig. 2a), as well as $V_{12}O_{40}H_{20}$ ($V_2O_9H_8$ + $V_{10}O_{31}H_{12}$) and $V_{20}O_{62}H_{24}$ ($V_{10}O_{31}H_{12}$ + $V_{10}O_{31}H_{12}$) clusters representing two layers (Fig. 2b). The electronic cluster calculations are carried out using the semiempirical ZINDO method. Table I summarizes the results for a V_2O_9 fragment in $V_2O_9H_{10}$ cluster with the bulk geometry, in $V_2O_9H_8$ cluster with the optimized geometry (V_2O_9 part optimized, H atoms kept in their positions), in $V_{10}O_{31}H_{12}$ cluster with the optimized V_2O_9 part, and for the two layers $V_{12}O_{40}H_{20}$ ($V_2O_9H_8$ + $V_{10}O_{31}H_{12}$) cluster, where the V_2O_9 part of the first layer is optimized. Similarly, Table II summarizes the results for the $V_{10}O_{31}$ fragment in $V_{10}O_{31}H_{12}$ cluster with its bulk geometry, in $V_{10}O_{31}H_{12}$ cluster with the optimized geometry ($V_{10}O_{31}$ optimized, H atoms are kept in their position), in $V_{24}O_{71}H_{12}$ cluster with the optimized $V_{10}O_{31}$ part, and for the two layer cluster $V_{20}O_{62}H_{24}$ ($V_{10}O_{31}H_{12}$ + $V_{10}O_{31}H_{12}$) where the $V_{10}O_{31}$ part from the first layer is optimized. For completion, Figs 3 and 4 illustrate the changes in geometry for both types of cluster.

The different optimizations of the cluster geometries do not significantly influence the electronic structure of the clusters (Tables I and II). The V–O bonds are characterized by ionic and covalent contributions. The ionic part is reflected by the different atom charging in the system. The vanadium atom is always positive (+0.9 to +1.2)

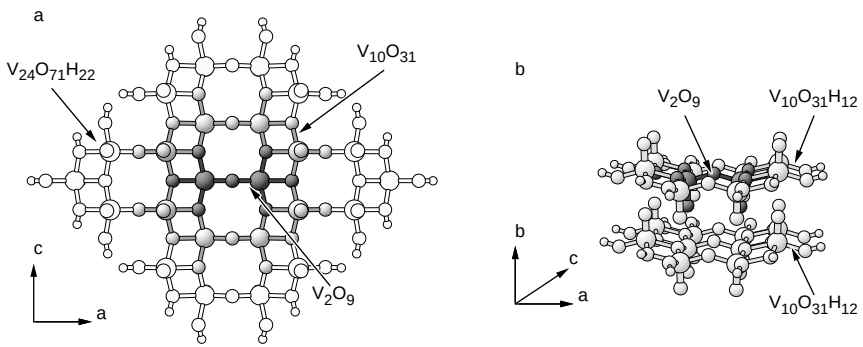

FIG. 2

Clusters used to model (010) surface of V_2O_5. a: $V_2O_9H_8$, $V_{10}O_{31}H_{12}$, $V_{24}O_{71}H_{12}$ clusters accounting for one layer; the black balls refer to V_2O_9 fragment, the shaded to $V_{10}O_{31}$ fragment, whereas the white ones to $V_{24}O_{71}H_{12}$ cluster. b: $V_{12}O_{40}H_{20}$ ($V_2O_9H_8$ + $V_{10}O_{31}H_{12}$) and $V_{20}O_{62}H_{24}$ ($V_{10}O_{31}H_{12}$ + $V_{10}O_{31}H_{12}$) clusters representing two layers, the black balls refer to V_2O_9 fragment. Note that H terminator atoms are included only for the largest cluster

TABLE I

Results of Mulliken population analyses as well as geometry optimizations for the different V_2O_9 fragments. The second column refers to $V_2O_9H_8$ cluster with bulk geometry, the third to the $V_2O_9H_8$ cluster with optimized V_2O_9 fragment, the next to the $V_{10}O_{31}H_{12}$ cluster with optimized V_2O_9 fragment, the last one to the $V_{12}O_{40}H_{20}$ ($V_2O_9H_8$ + $V_{10}O_{31}H_{12}$) cluster with optimized V_2O_9 fragment in the first layer. The atom charges Q, refer to vanadium and oxygen atoms closest to the cluster center. For each type of oxygen (singly coordinated O(a), doubly coordinated O(b,c) and triply coordinated O(d,e)) P_{V-O} denotes the bond order with the nearest vanadium atom and R_{V-O} are appropriate distances. Quantities ∢V–O(c)–V and ∢O(a)–V–O(b,c) refer to the angles between vanadium atoms and oxygen centers. The total energies are in a.u., ∢V–O–V angles in degrees, and distances in Å

Calculated quantities	$V_2O_9H_8$ no opt	$V_2O_9H_8$ V_2O_9 opt	$V_{10}O_{31}H_{12}$ V_2O_9 opt	$V_{12}O_{40}H_{20}$ no opt	$V_{12}O_{40}H_{20}$ V_2O_9 opt
Energy	–167.1074	–167.2535	–582.2389	–749.1253	–749.2637
Q_V	1.22	1.07	0.93	1.25	.10
$Q_{O(a)}$	–0.42	–0.37	–0.33	–0.43	–0.39
$Q_{O(b,c)}$	–0.47	–0.44	–0.44	–0.47	–0.43
$R_{V-O(a)}/P_{V-O(a)}$	1.59/2.49	1.59/2.58	1.59/2.60	1.59/2.38	1.61/2.41
$R_{V-O(b,c)}/P_{V-O(b,c)}$	1.78/1.22 1.78/1.22	1.92/1.17 1.92/1.17	1.95/0.95 1.80/1.43	1.78/1.22 1.78/1.22	1.92/1.17 1.92/1.17
∢O(a)–V–O(b,c)	104.79	109.08	110.89	104.79	108.59
∢V–O(b,c)–V	148.17	140.47	170.54	148.17	132.96

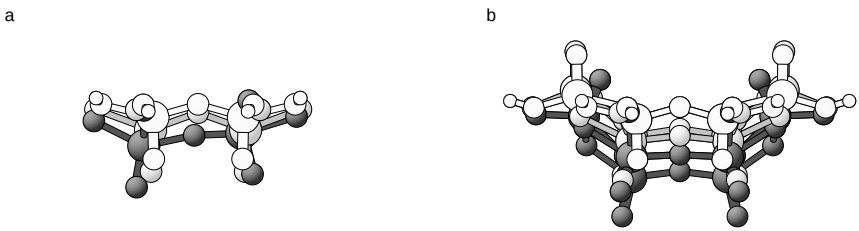

FIG. 3

Geometric structures obtained after the optimization. a: $V_2O_9H_8$ cluster; white balls refer to V_2O_9 fragment with the bulk structure, light shaded to optimized V_2O_9 part of $V_2O_9H_8$ cluster and black ones to the optimized V_2O_9 being the fragment of the larger $V_{10}O_{31}H_{12}$ cluster; view along the (001) direction. b: $V_{10}O_{31}H_{12}$ cluster; white balls refer to $V_{10}O_{31}$ fragment with the bulk structure, light shaded to optimized $V_{10}O_{31}$ part of $V_{10}O_{31}H_{12}$ cluster and black ones to the optimized $V_{10}O_{31}$ fragment of the larger $V_{24}O_{71}H_{22}$ cluster; view along the (001) direction

whereas all oxygen sites form negative ions. Both types of bridging oxygens (coordinated to two and to three vanadium atoms) carry a little more negative charge than the terminal vanadyl oxygen sites. The geometry optimization leads in general to a less pronounced difference in charges between vanadium and oxygen atoms. The covalent contributions are described by the respective bond order indices P_{V-O}. The value of $P_{V-O(a)}$ describing the bond of a vanadium atom with its terminal oxygen amounts to

TABLE II

Results of Mulliken population analyses as well as geometry optimizations for the different $V_{10}O_{31}$ fragments. The second column refers to $V_{10}O_{31}H_{12}$ cluster with bulk geometry, the third to the $V_{10}O_{31}H_{12}$ cluster with optimized $V_{10}O_{31}$ fragment, the next to the $V_{24}O_{71}H_{22}$ cluster with optimized $V_{10}O_{31}$ fragment, the following to the non optimized $V_{20}O_{62}H_{24}$ ($V_{10}O_{31}H_{12}$ + $V_{10}O_{31}H_{12}$) cluster, and the last one to the $V_{20}O_{62}H_{24}$ ($V_{10}O_{31}H_{12}$ + $V_{10}O_{31}H_{12}$) cluster with optimized $V_{10}O_{31}$ fragment in the first layer. The atom charges Q, refer to vanadium and oxygen atoms closest to the cluster center. For each type of oxygen (singly coordinated O(a), doubly coordinated O(b,c) and triply coordinated O(d,e)) P_{V-O} denotes the bond order with the nearest vanadium atom and R_{V-O} are appropriate distances. Quantities ∢V–O(c)–V, ∢O(a)–V–O(b,c) and ∢O(b,c)–V–O(d,e) refer to the angles between vanadium atoms and oxygen centers. The total energies are in a.u., ∢V–O–V angles in degrees, and distances in Å

Calculated quantities	$V_{10}O_{31}H_{12}$ no opt	$V_{10}O_{31}H_{12}$ $V_{10}O_{31}$ opt	$V_{24}O_{71}H_{22}$ $V_{10}O_{31}$ opt	$V_{20}O_{62}H_{24}$ no opt	$V_{20}O_{62}H_{24}$ $V_{10}O_{31}$ opt
Energy	–581.9343	–582.7404	–1336.1635	–1164.1146	–1164.8649
Q_V	1.09	0.94	0.96	1.09	0.94
	1.16	1.02	0.94	1.16	1.03
	1.17	1.02	0.93	1.20	1.05
$Q_{O(a)}$	–0.38	–0.34	–0.34	–0.39	–0.36
$Q_{O(b,c)}$	–0.46	–0.43	–0.43	–0.46	–0.41
$Q_{O(d,e)}$	–0.48	–0.41	–0.41	–0.48	–0.41
$R_{V-O(a)}/P_{V-O(a)}$	1.59/2.49	1.58/2.61	1.58/2.62	1.59/2.42	1.60/2.47
$R_{V-O(b,c)}/P_{V-O(b,c)}$	1.78/1.21	1.90/1.19	1.93/1.16	1.78/1.22	1.91/1.17
	1.78/1.21	1.90/1.19	1.93/1.16	1.78/1.22	1.91/1.17
$R_{V-O(d,e)}/P_{V-O(d,e)}$	1.88/0.91	2.09/0.87	2.09/0.84	1.88/0.92	2.06/0.89
	1.88/0.85	2.11/0.84	2.04/0.94	1.89/0.97	2.07/0.86
	2.02/0.68	2.23/0.68	2.25/0.60	2.02/0.65	2.21/0.64
∢O(a)–V–O(b,c)	104.79	112.74	110.50	104.79	110.87
∢O(b,c)–V–O(d,e)	97.02	96.44	94.25	97.02	93.50
∢V–O(b,c)–V	148.17	162.19	165.70	148.17	138.93

about 2.5, confirming the strong vanadyl double bond. The value of the bond order $P_{V–O(b,c)}$ characterizing the bond of a doubly coordinated oxygen with each of its nearest vanadium atoms, is found to be about 1.1 which indicates two single V–O bonds. Furthermore, the bond order $P_{V–O(d,e)}$ representing the bond between triply coordinated oxygen and its neighboring vanadiums yields a value of about 0.8 suggesting three bonds that are weaker than a single bond.

Different optimization procedures (various boundary conditions assumed during the optimization) lead to significant changes in the geometries of the clusters. Generally, the bond distances between vanadium and bridging oxygen atoms become elongated; for doubly coordinated O(b,c) oxygen atoms from 1.78 to 1.95 Å, and for triply coordinated O(d,e) oxygen atoms from 1.88 to 2.25 Å (Tables I and II). Also, the angles between the different oxygen and vanadium atoms change such that the bridging oxygen atoms move out of the surface in the direction of the nearest vanadyl groups. These changes in the geometric structure of the clusters are illustrated in Figs 3 and 4.

The optimized geometry of the cluster remains much closer to the surface geometry (represented by the white balls, Fig. 3) when the optimization is done for the whole cluster, V_2O_9 in $V_2O_9H_{12}$ or $V_{10}O_{31}$ in $V_{10}O_{31}H_{12}$, (see shaded balls, Fig. 3) excluding the saturated hydrogen atoms. Optimization of the inner fragment of the cluster, V_2O_9 in $V_{10}O_{31}H_{12}$ cluster or $V_{10}O_{31}$ in $V_{24}O_{71}H_{12}$ cluster, (see black balls, Fig. 3), results in a significant rearrangement of the cluster structure and lead to a “warped” geometry (bridging oxygen as well as vanadium atoms are shifted out of the surface). This indicates that hydrogen atoms preserve the surface geometry more effectively than the nearest environment of the local surface cluster (simulated by the bigger cluster). The

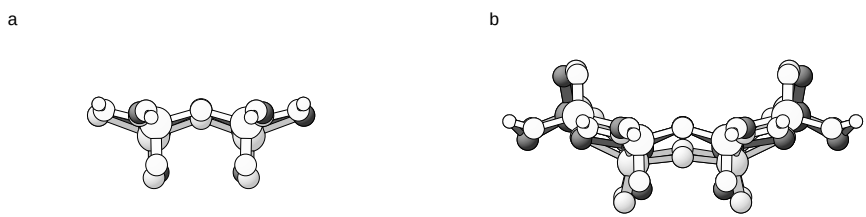

FIG. 4

Geometric structures obtained after the optimization. a: $V_2O_9H_8$ cluster; white balls refer to V_2O_9 fragment with the bulk structure, light shaded to optimized V_2O_9 part of $V_2O_9H_8$ cluster and black ones to the optimized V_2O_9 being the first layer of the two layers $V_{12}O_{40}H_{20}$ ($V_2O_9H_8$ + $V_{10}O_{31}H_{12}$) cluster; view along the (001) direction. b: $V_{10}O_{31}H_{12}$ cluster; white balls refer to $V_{10}O_{31}$ with the bulk structure, light shaded to optimized $V_{10}O_{31}$ part of $V_{10}O_{31}H_{12}$ cluster and black ones to the optimized $V_{10}O_{31}$ being the first layer of the two layers $V_{20}O_{62}H_{24}$ ($V_{10}O_{31}H_{12}$ + $V_{10}O_{31}H_{12}$) cluster; view along the (001) direction

presence of the second layer corrects the geometry changes following on from the optimization procedure. Figure 4a compares the structures of the V_2O_9 fragment in $V_2O_9H_{12}$ cluster in bulk geometry (white balls) with its optimized geometry (H atoms kept frozen) (shaded balls) as well as with V_2O_9 geometry optimized in the $V_{12}O_{40}H_{20}$ cluster *i.e.* in the presence of the second layer (black balls). A similar summary of the optimizations of the $V_{10}O_{31}$ fragment performed with different boundary conditions is shown in Fig. 4b.

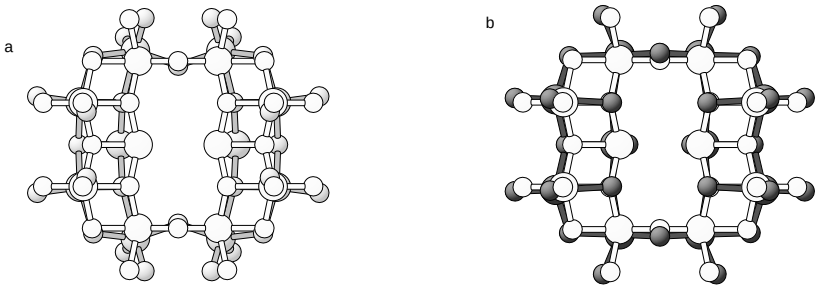

FIG. 5
Vacancy formation by removing the doubly coordinated bridging oxygen O(c); view along the (010) direction. a: Optimized geometric structures for $V_{10}O_{30}$ fragment (shaded balls) of $V_{10}O_{31}H_{12}$ cluster; white balls refer to $V_{10}O_{30}$ fragment with the bulk structure. b: Optimized geometric structures for $V_{10}O_{30}$ fragment (black balls) being the first layer of the two layers $V_{20}O_{61}H_{24}$ ($V_{10}O_{30}H_{12}$ + $V_{10}O_{31}H_{12}$) cluster; white balls refer to $V_{10}O_{30}$ fragment with the bulk structure

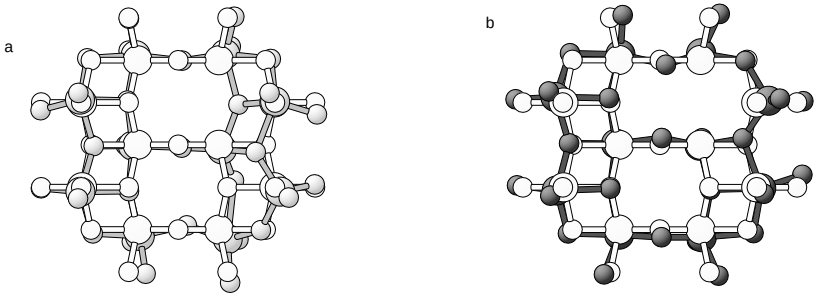

FIG. 6
Vacancy formation by removing the triply coordinated bridging oxygen O(d); view along the (010) direction. a: Optimized geometric structures for $V_{10}O_{30}$ fragment (shaded balls) of $V_{10}O_{31}H_{12}$ cluster; white balls refer to $V_{10}O_{30}$ fragment with the bulk structure. b: Optimized geometric structures for $V_{10}O_{30}$ fragment (black balls) being the first layer of the two layers $V_{20}O_{61}H_{24}$ ($V_{10}O_{30}H_{12}$ + $V_{10}O_{31}H_{12}$) cluster; white balls refer to $V_{10}O_{30}$ fragment with the bulk structure

Two types of the boundary conditions assumed during the optimization process lead to similar results, the optimization of all atoms in the cluster (with saturating hydrogen atoms kept frozen) and the same optimization in the presence of the second layer. They also lower the cluster energies by the same amount, in the case of V_2O_9 fragment by 0.15 and 0.14 a.u. for $V_2O_9H_8$ and $V_{12}O_{40}H_{20}$ (two layers) clusters, in the case of $V_{10}O_{31}$ fragment by 0.81 and 0.75 a.u. for $V_{10}O_{31}H_{12}$ and $V_{20}O_{62}H_{24}$ (two layers) clusters.

Electronic and Geometric Structures of V_2O_5 Surface Clusters with Oxygen Vacancy

In a catalytic oxidation process surface oxygen atoms participate in the reaction by activating the hydrocarbon molecules (splitting of C–H bonds) and by being incorporated into organic molecules (formation of C–O bonds). As a consequence, a series of oxygen vacancies is created which may undergo reoxidation by gaseous oxygen or may lead to the rearrangement of V–O bonds and formation of the crystallographic sheare plane. In the interaction of a single hydrocarbon molecule with the surface cluster only one oxygen vacancy is formed. Therefore no significant change in the surface geometry is expected. Since all previous calculations suggest the bridging surface oxygen atom as that which oxygenates the hydrocarbon molecule, we have performed geometry optimization for $V_{10}O_{30}$ fragments (in one layer $V_{10}O_{31}H_{12}$ and two layer $V_{20}O_{62}H_{24}$ clusters) with the oxygen vacancy created in bridging positions, by taking away the doubly O(c) and triply O(d) coordinated bridging oxygen atoms from the respective clusters. The results of the different optimizations for the $V_{10}O_{30}$ fragment are shown in Figs 5 and 6, for vacancies formed at O(c) and O(d) positions, respectively. One can notice a significant change in $V_{10}O_{30}$ geometry for the case in which this fragment is optimized without the second layer (shaded balls). There are changes in distances (see clusters plotted along (010) direction, Figs 5 and 6, shaded balls), and in addition clusters get warped shapes. In the case of the formation of O(d) vacancies there is a reconstruction of the cluster, namely one of the vanadyl oxygen leaves its normal position and refills the vacancy (takes a position of the triply coordinated bridging oxygen (Fig. 6, shaded balls). The optimization carried out for $V_{10}O_{30}$ fragments being the first layer of two layer $V_{20}O_{62}H_{24}$ cluster, and obtained by creating the vacancy at O(c) or O(d) positions, leads to small changes in the geometric structure of the cluster (black balls). The presence of the second layer protects the rearrangement of the cluster and the refilling of the vacancy by vanadyl oxygen does not take place.

CONCLUSIONS

The present cluster model calculations confirm the electronic structure and binding at the (010) surface of a vanadium pentoxide which was found previously[3–17]. All electronic parameters of the $V_{10}O_{31}H_{12}$ cluster in its bulk and optimized geometry are found to be similar. The electronic binding in vanadium pentoxide is described by both ionic

and covalent contributions. The calculations reveal clear electronic differences between structurally different surface oxygen sites. Bridging oxygen sites are always found to be more negatively charged than terminal (vanadyl) oxygen sites, which suggests an increased local reactivity of bridging oxygen centers with respect to electrophilic attacks. The present calculations indicate that hydrogen atoms preserve the surface geometry more effectively than the nearest environment of the local surface cluster simulated by the bigger cluster. The presence of the second layer corrects the geometry changes following on from the optimization procedure and stabilizes the surface geometry. In contrast to recent SINDO semiempirical calculations[29] the second layer is found to have no influence on the electronic structure of V_2O_5 (010) surface but to play a significant role in the geometry optimization. The formation of an oxygen surface vacancy in bridging position (both doubly and triply coordinated) results in significant changes in local geometry for one layer clusters. The presence of the second layer preserve the bulk geometry and the creation of the oxygen vacancy at bridging position is connected with only small changes in surface geometry.

REFERENCES

1. Grzybowska-Swierkosz B., Haber J. (Eds): *Vanadia Catalysts for Processes of Oxidation of Aromatic Hydrocarbons*. PWN – Polish Scientific Publishers, Warsaw 1984.
2. Bielanski A., Piwowarczyk J., Pozniczek J.: *J. Catal.* **1988**, *113*, 334.
3. Witko M., Hermann K.: *J. Mol. Catal.* **1993**, *81*, 279.
4. Witko M., Hermann K. in: *Studies in Surface Science and Catalysis* (S. V. Bellon and V. C. Corberan, Eds), Vol. 82, p. 75. Elsevier, Amsterdam 1994.
5. Witko M., Hermann K., Tokarz R.: *J. Electron. Spectrosc. Relat. Phenom.* **1994**, *69*, 89.
6. Hermann K., Michalak A., Witko M.: *Catal. Today* **1996**, *32*, 321.
7. Michalak A., Witko M., Hermann K.: *Surf. Sci.* **1997**, *375*, 385.
8. Hermann K., Witko M., Druzinic R., Chakrabarti A., Tepper B., Elsner M., Gorschluter A., Kuhlenbeck H., Freund H.-J.: *J. Electron. Spectrosc. Relat. Phenom.*, in press.
9. Witko M., Tokarz R., Haber J.: *J. Mol. Catal.* **1991**, *66*, 205.
10. Witko M., Tokarz R., Haber J.: *J. Mol. Catal.* **1991**, *66*, 357.
11. Witko M.: *Catal. Today* **1996**, *32*, 89.
12. Witko M., Tokarz R., Haber J.: *J. Appl. Catal. A* **1997**, *157*, 23.
13. Witko M., Tokarz R., Hermann K.: *Pol. J. Chem.*, in press.
14. Witko M., Hermann K., Tokarz R., Michalak A.: *ACS Symp. Ser.* **1997**, *42*, 94.
15. Nalewajski R. F., Korchowiec J., Tokarz R., Broclawik E., Witko M.: *J. Mol. Catal.* **1992**, *77*, 165.
16. Nalewajski R. F., Korchowiec J.: *J. Mol. Catal.* **1993**, *82*, 383.
17. Chakrabati A., Hermann K., Druzinic R., Witko M., Wagner F., Petersen M.: Unpublished results.
18. Hermann K., Bagus P. S., Nelin C. J.: *Phys. Rev. B: Solid State* **1987**, *35*, 9467.
19. Chelikowski J. R., Schlter M., Louie S. G, Cohen M. L.: *Solid State Commun.* **1975**, *17*, 1103.
20. Szabo A., Ostlund N. S.: *Modern Quantum Chemistry: Introduction to Advanced Electronic Structure Theory*. Macmillian, New York 1992.

21. Labanowski J. K., Andzelm J. W. (Eds): *Density Functional Methods in Chemistry*. Springer, Heidelberg 1991.
22. Sadlej J.: *Semi-Empirical Methods of Quantum Chemistry CNDO, INDO, NDDO*. PWN – Polish Scientific Publishers, Warszaw and Ellis Horwood, Chichester 1985.
23. Bystrom A., Wilhelmi K. A., Brotzen O.: *Acta Chem. Scand.* **1950**, *4*, 1119.
24. Bachman H. G., Ahmed F. R., Barnes W. H.: *Z. Kristallogr. Kristallgeom. Kristallphys. Kristallchem.* **1981**, *115*, 110.
25. Wyckoff R. W. G.: *Crystal Structures*. Wiley, New Yorkd 1965.
26. Zerner M. C., Loew G. H., Kirchner R. F., Muller-Westerhoff U. T.: *J. Am. Chem. Soc.* **1980**, *102*, 589.
27. Bacon A. D., Zerner M. C.: *Theor. Chim. Acta* **1979**, *53*, 21.
28. Edwards W. D., Zerner M. C.: *Theor. Chim. Acta* **1987**, *72*, 347.
29. Zhanpeisov N. U., Bredow T., Jug K.: *Catal. Lett.* **1996**, *39*, 111.